THE INTERPRETATION OF MULTI-WAVELENGTH SPECTRA IN SNR G347.3−0.5 (RX J1713.7−3946)

M. G. Baring
Rice University
Department of Physics and Astronomy
6100 Main St., Houston, TX 77251
BARING@RICE.EDU

Abstract

The recent CANGAROO detection of TeV γ-rays from the southern hemisphere remnant RX J1713.7−3946 (G347.3−0.5) has spawned a debate over whether this data provides evidence for the production of cosmic ray ions in this source. The discovery paper of Enomoto et al. argued against an inverse Compton origin for these photons from a population of electrons that generates radio to X-ray synchrotron emission. Such conclusions were predicated on a limited test-particle (linear) model for shock acceleration. Non-linear models of acceleration are widely regarded as appropriate for remnant shells, and generate multi-wavelength spectra that can differ significantly from test-particle predictions. This paper explores such non-linear models and the expectations for radio/X-ray synchrotron spectra, and inverse Compton γ-ray spectra. It is found that reasonable values of environmental parameters such as density and magnetic field strength, adjusted only modestly from the previous analysis of Ellison et al., can yield acceptable fits to the radio, X-ray, and TeV fluxes and spectra, and can accommodate the constraining bounds imposed by a proximate unidentified *EGRET* source.

1 Introduction

The supernova remnant RX J1713.7−3946 (ROSAT designation; the radio designation is G347.3−0.5) has recently been the subject of controversy, following the publication of Atmospheric Cherenkov Telescope detections by the CANGAROO telescope in Australia, announced in Enomoto, et al. (2002).

Enomoto et al. reported a steeply falling flux in the TeV band, and claimed it as evidence for the generation of cosmic rays in this source. The basis for their assertions was that they could perform a multi-wavelength fit using radio data published in Ellison, Slane and Gaensler (2001), and ASCA data (see Enomoto et al. 2002 for references), and achieve attractive fits to these three bands with a prominent neutral pion decay component from collisions of SNR-accelerated cosmic rays and ambient protons. Enomoto et al. claimed that the inverse Compton signal peaking in the TeV could not fit the data, whereas the pion-decay curve can.

Reimer and Pohl (2002) and Butt et al. (2002) introduced data from a proximate *EGRET* unidentified source into the discussion, and indicated that this data could be conservatively taken as upper bounds to interpretative models, thereby ruling out Enomoto et al.'s (2002) contention of the presence of the signature of cosmic rays.

This debate has been fueled by models that used test particle acceleration models. Ellison et al. (2001) used a more appropriate non-linear acceleration treatment on this source, with the conclusion of a strong inverse Compton dominance in the TeV band. The refined CANGAROO TeV data in Enomoto et al. (2002) requires an update of the non-linear investigations. Here we provide such, with a multi-wavelength approach that hinges on the radio and X-ray data to establish constraints.

2 Non-linear acceleration

Non-linear acceleration studies have led to an approximate consensus concerning the shape of the ion distribution; results from semi-analytic and Monte Carlo models are quite similar (Berezhko & Ellison 1999). This has led to the generation of a simplified analytic description of resultant ion distributions, that

was extended to treat electron distributions in Ellison, Berezhko & Baring (2000).

The characteristic signatures of non-linear acceleration that impact radiative spectral diagnostics include concavity in the distribution that signals departures from test-particle power-law behavior, and cooler sub-shock temperatures due to hydrodynamic modifications that can critically influence the interpretation of X-ray line features.

The distinctive concavity is illustrated in Fig. 1, where analytic models and a Monte Carlo simulation of the non-linear acceleration problem are compared. The analytic model suffices as an expedient tool for radiative considerations in astrophysics.

The mathematical form for the approximate proton spectrum is obtained in Berezhko & Ellison (1999; see also Ellison, Berezhko and Baring 2000):

$$f(p) = \begin{cases} a_{\rm inj}\,(p/p_{\rm inj})^{-q_{\rm sub}} & \text{if} \quad p_{\rm inj} \le p \le m_p c, \\ a_{\rm mc}\,[p/(m_p c)]^{-q_{\rm int}} & \text{if} \quad m_p c \le p \le p_{01}, \\ a_{\rm max}\,(p/p_{01})^{-q_{\rm min}} & \text{if} \quad p_{01} \le p \le p_{\rm max}. \end{cases} \tag{1}$$

Here, $q_{\rm sub}$ is determined by the sub-shock compression ratio

$$q_{\rm sub} = \frac{3r_{\rm sub}}{r_{\rm sub}-1} \quad , \tag{2}$$

$q_{\rm min}$ is given by,

$$q_{\rm min} = \frac{7}{2} + \frac{7-r_{\rm sub}}{2(2r_{\rm tot}-r_{\rm sub}-1)} \quad . \tag{3}$$

The remaining index at intermediate energies, $q_{\rm int}$, is formed from an arithmetic mean of $q_{\rm min}$ and the test particle index appropriate for the upstream gas conditions, i.e., is dependent on the sonic Mach number of the upstream gas. The normalization factors a in Eq. (1) are simply related using continuity of the distribution, and can be expressed in terms of a parameter $\eta_{\rm inj,p}$ that specifies the rate of proton injection from the thermal pool.

The non-linear distribution can be determined with four arbitrary parameters: (1) $p_{\rm inj}$, (2) the rate of proton injection, $\eta_{\rm inj,p}$, (3) the maximum momentum, $p_{\rm max}$, where the spectrum cuts off, and (4) p_{01}. The results are relatively insensitive to p_{01}, which we take as $p_{01} = \min\{0.01 p_{\rm max}, m_p c\}$.

The hydrodynamics are controlled by the massive ions, so that the electrons just go along for a diffusive ride,

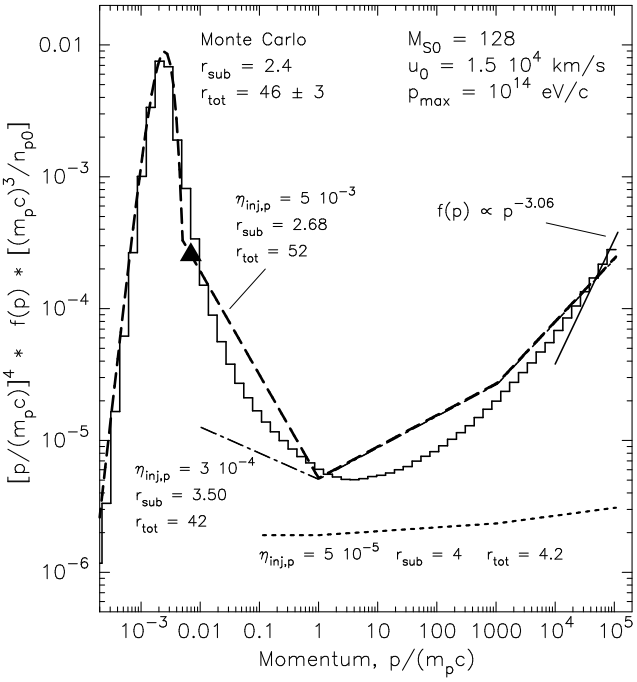

Figure 1: Downstream proton momentum phase space distributions for diffusive acceleration at a modified shock. The figure is taken from Ellison, Berezhko and Baring (2000), where the simple analytic model is described in detail. The dashed and dash-dotted curves are two simple non-linear models with different proton injection parameters $\eta_{\rm inj,p}$ as labeled. The histogram is an exact non-linear Monte Carlo simulation for the same shock parameters.

sampling the flow velocity spatial profile established by the ions. Once the electrons are relativistic, their acceleration distribution can be equated to that for those protons of comparable diffusive scale, i.e., rigidity or momentum. This leads to a very simple approximate tracing of distributions (see Ellison, Berezhko and Baring 2000):

$$f_e(p) = K_{ep} f_p(p) \quad , \quad K_{ep} = \frac{a_{\rm inj,e}}{a_{\rm inj,p}} \left(\frac{p_{\rm inj,e}}{p_{\rm inj,p}} \right)^{q_{\rm sub}} \quad . \tag{4}$$

The electron injection efficiency parameter is not explicitly specified, and can be obtained from the relative normalization of the proton and electron distributions, coupling to the the electron-to-proton temperature ratio T_e/T_p, which encapsulates the degree of electron heating in the sub-shock, and the relativistic e/p abundance ratio, which is set in the range 0.01–0.05 to match measured cosmic ray abundances. Details are given in Ellison, Berezhko and Baring (2000).

Hence, the inclusion of electrons essentially yields

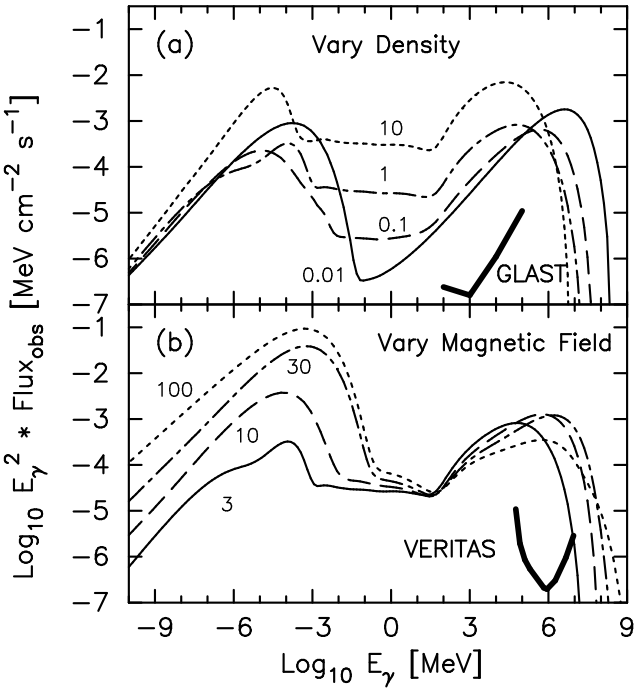

Figure 2: Broadband spectral templates from the simple analytic model of Ellison, Berezhko and Baring (2000), including several radiation components (see text). The two panels depict the impacts of varying the ambient density in the range 0.01–10 cm^{-3}, and the ambient upstream magnetic field from 3 μG to 100 μG, as indicated.

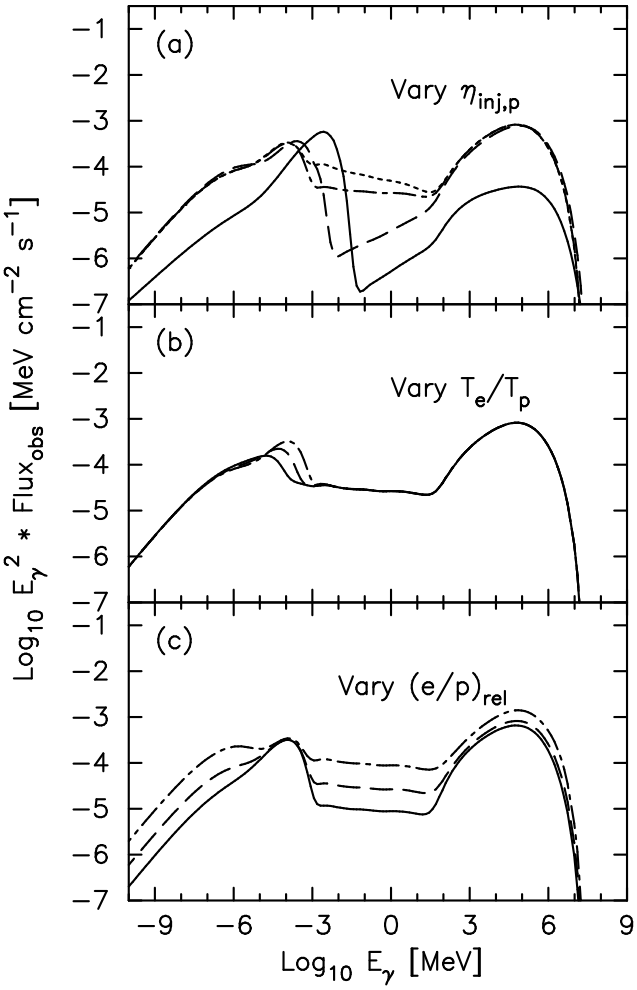

Figure 3: Broadband spectral templates as in Fig. 2. The three panels depict the impacts of varying the proton injection parameter $\eta_{\rm inj,p}$, the electron-to-proton temperature ratio T_e/T_p, and the relativistic e/p abundance ratio, as indicated.

only two additional parameters. The pool of parameters can be directly coupled SNR environmental parameters such as the energy of the ejecta, the ambient density of matter, and the field strength in the unshocked flow. We use here the relationships established by Ellison, Slane and Gaensler (2001), though alternative possibilities for generic SNRs are offered by Baring et al. (1999). Such a simplified analytic model is extremely facile for generating predictions of photon emission spectra in supernova remnants.

3 Photon spectra and interpretation

Sample photon spectra that display the correlations between spectral behavior and parametric input are given in Fig. 2 and 3. In both figures the following radiation components are included: synchrotron in the downstream field, inverse Compton off the microwave background, $e-p$ and $e-e$ bremsstrahlung, and pion decay emission from collisions between cosmic rays and ambient protons. The analytic forms of the electron and proton distributions admit development of analytic forms for synchrotron and inverse Compton emissivities; this is not possible for bremsstrahlung and pion decay rates.

In Fig. 2, it is clear that low density models yield prominent inverse Compton components in the TeV band, whereas high density ones $n \gtrsim 1$ cm^{-3} permit the appearance of a π^0 decay bump in the sub-GeV band. Further, the increase in density slows the shocked shell faster and so reduces the maximum energy of acceleration.

Moreover, increasing the ambient magnetic field not only renders the radio-to-X-ray synchrotron component much more prominent, but weakens the shock to reduce the non-linear curvature of the distribution, and so reduces the γ-ray signal. At the same time, the diffusive scales are smaller so that acceleration persists to

higher energies, hardening the TeV prediction.

Trends in Fig. 3 are as follows: higher T_e/T_p naturally generates harder X-ray emission, but this ratio is otherwise not influential. Greater relativistic e/p abundance ratios obviously generate more radio-to-X-ray synchrotron and hard X-ray/soft γ-ray bremsstrahlung.

More importantly, increasing the proton injection parameter $\eta_{\rm inj,p}$ profoundly changes the non-linearity of the shock, steepening the distribution of the lower electrons (and so increasing the bremsstrahlung contribution), enhancing the number of highest energy particles (thereby brightening the γ-ray band) and cooling the gas in the sub-shock region so as to reduce the X-ray hardness.

Results are depicted for ambient densities of n_p = 1 cm^{-3}, higher than those appropriate for SNR G347.3−0.5. Nevertheless, they serve to illustrate the main effects.

3.1 SNR G347.3−0.5

Here, parameters chosen for this source are similar to those adopted by Ellison, Slane and Gaensler (2001), yet they differ in significant ways. The environment of the remnant suggests that there is an evacuated density within the shell, i.e., it is well below n_p = 1 cm^{-3}. This renders *pp* collisions ineffective, so that only synchrotron and inverse Compton emission need be considered at this juncture.

Considerations of adjacent molecular clouds as targets for pion production would mandate the use of much higher target densities for the pion decay emission, but will be the subject of future work; the present models will represent the radio to X-ray band well, and will provide a significant contribution to γ-ray emission.

The CANGAROO data presented in Enomoto et al. (2002) postdate the preliminary data used by Ellison, Slane and Gaensler (2001), and are significantly more constraining, requiring a spectral turnover in the sub-TeV band. To effect this, we imposed a lower $\gamma_{\rm max,e}$ for the electrons (and protons), since this controls the inverse Compton peak.

There are two main ways to accomplish this: decrease B, or increase the ratio λ/r_g of the diffusive mean free path λ to the gyroradius r_g of particles. However, the synchrotron peak must remain just below the X-ray band, requiring $\gamma^2_{\rm max,e}B$ to be held constant.

Here we opted to depart from the Bohm diffusion assumption of Ellison, Slane and Gaensler (2001) and obtained $\lambda/r_g \sim 10$ and increased the upstream field by around a factor of 4–5 from their model A (i.e., lowering it from their model C).

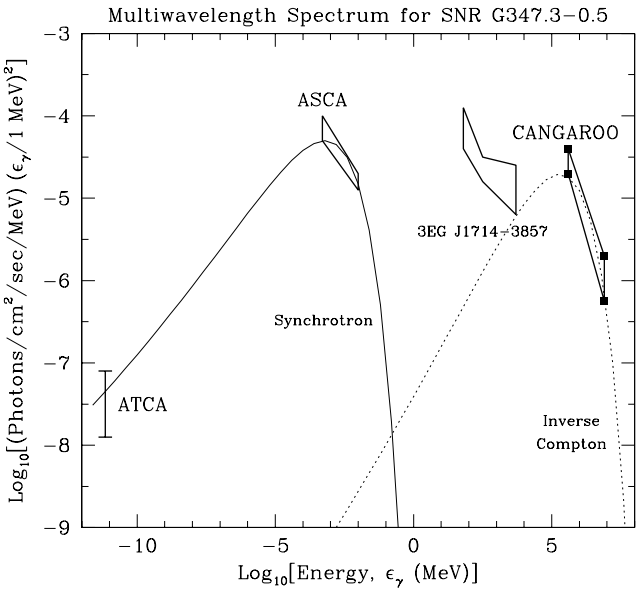

Figure 4: Multi-wavelength spectral model for SNR G347.3−0.5 (RX J1713.7−3946) from the simple analytic model of Ellison, Berezhko and Baring (2000). The spectrum is appropriate for low density shells and therefore includes only synchrotron and inverse Compton components. The constraining CANGAROO data above 1 TeV required lowering of the maximum acceleration energy below that used by Ellison, Slane and Gaensler (2001). Also depicted are the ATCA radio data, *ASCA* X-ray spectrum, and the unidentified *EGRET* source 3 EG J1714−3857.

Spectral results are depicted in Fig. 4, to compare with the results of Enomoto et al. (2002) and Reimer & Pohl (2002). The model is moderately commensurate with the data, though *it requires* $\lambda/r_g > 1$. Other parameters were B_0 = 12 μG, n_p = 0.03 cm^{-3}, $(e/p)_{\rm rel}$ = 0.03 and $\gamma_{\rm max,e}$ = 2 TeV.

The fit can accommodate bounds imposed by the *EGRET* source, but cannot explain it. Hence, should *GLAST* confirm that the *EGRET* source is physically connected to the shell, or to a region that is energized by cosmic rays accelerated at the shell, a hadronic collisional scenario is the most promising likelihood. Otherwise, a leptonic explanation is the simpler choice to accommodate the CANGAROO data.

We remark that the analysis of very recent *HESS* observations of G347.3−0.5 in the TeV band will prove critical to the discussion. Also, spatially-resolved X-

ray observations coupled with shock models with a variety of field obliquities may provide the next order of diagnostics in relating the X-ray and TeV γ-ray components/turnovers.

References

Baring, M. G., Ellison, D. C., Reynolds, S. P., Grenier, I. A., Goret, P. 1999, ApJ, 513, 311

Berezhko, E. G., Ellison, D. C. 1999, ApJ, 526, 385

Butt, Y. M., et al. 2002, Nature, 418, 499

Ellison, D. C., Berezhko, E. G., Baring, M. G. 2000, ApJ, 540, 292

Ellison, D. C., Slane, P., Gaensler, B. M. 2001, ApJ, 563, 191

Enomoto, R., et al. 2002, Nature, 416, 823

Reimer, O., Pohl, M. 2002, A&A Let., 390, L43